Journal of Luminescence 157 (2015) 149–157

Contents lists available at ScienceDirect

Journal of Luminescence

journal homepage: www.elsevier.com/locate/jlumin

Photoluminescence and structural properties of Si/SiC core–shell nanowires growth by HWCVD

Nur Fatin Farhanah Binti Nazarudin, Nurul Jannah Binti Mohd Noor, Saadah Abdul Rahman, Boon Tong Goh *

Low Dimensional Materials Research Centre (LDMRC), Department of Physics, Faculty of Science, University of Malaya, 50603 Kuala Lumpur, Malaysia

ARTICLE INFO

Article history:
Received 12 January 2014
Received in revised form
26 August 2014
Accepted 27 August 2014
Available online 6 September 2014

Keywords:
Core–shell nanowires
Metal nano-templates
Metal diffusion growth
HWCVD
GI-SWAXS
Photoluminescence

ABSTRACT

Si/SiC core–shell nanowires grown by hot-wire chemical vapor deposition were studied. Ni nanoparticles act as metal nano-templates to catalyze the growth of these core–shell nanowires. These nanowires were grown at different deposition pressures of 0.5 and 1 mbar. The nanowires showed a tapered-like morphology at deposition pressure 0.5 mbar. Increase in pressure to 1 mbar leads to a formation of agglomerated grains at the root of the nanowires. The results show that these nanowires consisted of crystalline Si core and amorphous SiC shell nanowires. Increase in pressure enhanced the formation of SiC phase in the shell of the nanowires. On the other hand, the formation of the agglomerated grains attributed to an increasing of the SiC phase at higher deposition pressure. The presence of Si and SiC nano-crystallites embedded within an amorphous matrix exhibited a room temperature PL emission in the range of 400–1000 nm. The effects of the deposition pressure on the optical and structural properties of the nanowires are also discussed.

1. Introduction

One dimensional (1D) semiconductor nanostructures such as nanowires and nanorods have attracted more and more attention recently, due to their applications in mesoscopic physics and in the building blocks of nanoscale devices [1–3]. As a most important semiconductor 1D nanostructure materials, Si nanostructures, such as nanowires and nanorods, are of great interests owing to their excellent structural [4–6], optical [7–9] and electrical [10] properties. These superior properties have made the Si nanowires achieve excellent performance in solar cells, lithium ion batteries and thermoelectric devices [11–13]. However, due to their intrinsic material properties such as weak mechanical stability and associated side reactions resulting from unprotected surfaces, single-phased nanomaterials cannot fulfill certain application requirements [14,15]. Cui and co-workers reported that a crystalline core–amorphous shell Si nanowires design has shown a significant enhancement in capacity/power rate and efficiency for lithium-ion batteries and solar cell respectively [16]. Ryu et al. [17] and Tang and Bando [18] presented an enhancement of field emission properties of SiC/SiO_x core–shell nanowires. Moreover, Lee group [19] demonstrated a great improvement of light absorption and photocatalytic capability of ZnO/Si hierarchical core–shell heterostructures. For the application in high-temperature and high-power electronics, and electromechanical systems, incorporation of SiC nanostructures into the Si nanowires as a core–shell nanowire therefore is expected to further enhance the properties of the core–shell nanowires due to SiC possess various superior properties of high mechanical stability, chemical inertness, high thermal stability and in a wide range of optical properties [20–22].

Hot-wire chemical vapor deposition (HWCVD) is one of the most promising techniques for low temperature, high deposition rate and large-area deposition for SiC based thin films materials [23–25]. The HWCVD has demonstrated a low-temperature deposition (around 300 °C) of cubic SiC thin films. In the HWCVD process, the decomposition of SiH_4/CH_4 molecules on filament surfaces at filament temperature above 2000 °C sufficiently generates higher densities of growth precursors (SiH_3 and CH_3) than plasma processes. Moreover, decomposition of high density of H radicals plays an important role in the low-temperature growth of nanocrystalline SiC thin films. Recent studies on the growth of Si nanowires by HWCVD demonstrated that this technique is a promising technique for the growth of novel 1D Si based nanostructures owing to the lower production cost and large-scale production capability [26–28]. The HWCVD has also been reported to enhance the growth rate of Si nanowires [29]. Moreover, as compared to the conventional plasma enhanced CVD (PECVD), the HWCVD does not utilized high energy ions thus is expected to produce a better crystallinity of the

* Corresponding author. Tel.: +603 79674147.
E-mail address: boontong77@yahoo.com (B.T. Goh).

http://dx.doi.org/10.1016/j.jlumin.2014.08.049
0022-2313/

nanowires [30]. In this work, we grown nickel (Ni)-catalyzed Si/SiC core–shell nanowires by HWCVD at deposition pressures of 0.5 and 1 mbar. The photoluminescence and structural properties of these nanowires were investigated using field emission scanning electron microscopy (FESEM), scanning transmission electron microscopy with energy dispersive X-ray spectroscopy (STEM/EDS) mappings, STEM/High Angle Annular Dark-Field (HAADF), Micro-Raman scattering spectroscopy, glancing-angle small and wide angle X-ray scattering (GI-SWAXS), Micro-photoluminescence (PL) spectroscopy. The growth of the nanowires was found to be significant for the nanowires prepared at low deposition pressure. Results of the PL emissions in relation to the structural properties of the nanowires are also discussed. Moreover, the effects of the deposition pressure on the PL and structural properties are briefly described.

2. Experiments

Si/SiC core–shell nanowires were prepared on Ni coated glass substrates by a home-built HWCVD system. The Ni film thickness of about 30 ± 5 nm was deposited on the heated glass substrates under a vacuum condition. Prior to deposition, the Ni films were treated by atomic hydrogen plasma for 10 min in order to form metal nano-islands. The substrate temperature, pressure, hydrogen flow-rate and radio-frequency (rf) power were fixed at 450 °C, 0.75 mbar, 100 sccm and 5 W respectively. During the deposition, the filament temperature and substrate temperature were fixed at 1900 and 450 °C respectively. The filament temperature was measured using a pyrometer model Reytek, Raynger 3i. The filament to substrate distance was fixed at 2 cm. The SiH_4, CH_4 and H_2 flow-rates were fixed at 1, 2 and 100 sccm respectively. The vacuum base pressure was achieved as low as 5×10^{-7} mbar for the deposition pressures of 0.5 and 1 mbar. The total deposition time was fixed for 5 min.

The FESEM images of the nanowires were obtained using a Hitachi SU 8000 SEM at low electron accelerating voltage of 2 kV. The elemental spectra of the nanowire were collected by EDS detector attached to the SEM (Bruker XFlash 6|100) at 15 kV. The working distances for the imaging and elemental spectra were fixed at 8 mm and 15 mm respectively. In the same machine, the STEM/bright field was carried out on the sample prepared on a copper grid (Lacey Formvar, 300 mesh), for EDS elemental mappings of the nanowire. Furthermore, the details of surface morphology and microstructure of the nanowire were investigated by means of a TEM (JEOL JEM-2100F) with an accelerating voltage of 200 kV at STEM/HAADF configuration. The Raman spectra of the nanowires were recorded using an InVia Raman microscope with a charge-coupled device detector and a grating of 2400 lines/mm. The argon ion laser with an excitation wavelength and laser power of 514 nm and 10 mW respectively was used. The same spectrometer for the Raman measurement was used to obtain the PL spectra of the nanowires at room temperature, by selecting the HeCd laser with an excitation wavelength and laser power of 325 nm and 5 mW respectively. The GI-SWAXS spectra of the nanowires were studied on the beam line (BL23A) at the Taiwan National Synchrotron Radiation Research Center. The electron storage ring was operated at energy of 1.5 GeV. The X-ray beam was selectively monochromated by a double Si (1 1 1) crystal monochromater with a high energy resolution ($\Delta E/E = 2 \times 10^{-4}$ eV/eV) under energy of 10 keV. The Q-range for SAXS and WAXS were fixed at 0.007–0.27 and 0.7–2 $Å^{-1}$ respectively.

3. Results and discussion

The surface morphologies of Ni-catalyzed Si/SiC core–shell nanowires grown by HWCVD at different deposition pressures are depicted in Fig. 1. As can be seen, most of the nanowires possess a tapered morphology with a vertical alignment for the nanowires grown at 0.5 mbar. The inset of Fig. 1(a) clearly illustrates the tapered morphology of the nanowires. It is estimated from the figure that the average length and diameter of these nanowires are 587 and 51 nm respectively. The tapering of the nanowires reveals a radial growth of nanowires which generally occurred in the CVD growth nanowires. The radial growth of the nanowires by HWCVD has been extensively described elsewhere [31–33]. The nanowires prepared at 1 mbar shows a significantly decrease in length and diameter of the nanowires. The roots of these nanowires are surrounded by agglomerated grains. The formation of the agglomerated grains at higher deposition pressure can be due to the increase in gas phase reaction in HWCVD [34]. The enhancement of the gas phase reaction leads to a lateral growth thus induces the formation of the agglomerated grains at the roots of the nanowires. The formation of the agglomerated grains is clearly illustrated in the inset of the corresponding figure.

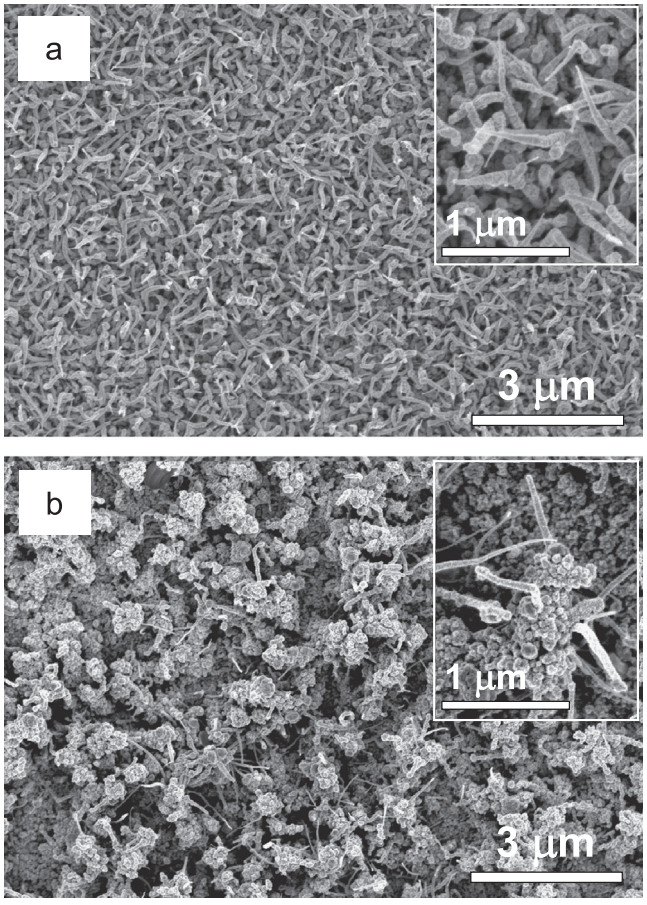

Fig. 1. FESEM images of Si/SiC core–shell nanowires prepared by HWCVD at different deposition pressures of (a) 0.5 and (b) 1 mbar. Insets of each figure present a high magnification of the respective FESEM images.

Table 1
Compositions of silicon, carbon, oxygen and nickel (in percentage) of the nanowires measured by EDS elemental analysis.

Pressure (mbar)	Nanowire	Si	C	O	Ni
0.5	Tip	63.9	2.8	15.3	11.8
	Stem	63	5.5	16.3	10.9
1	Tip	54.6	12.7	8.9	19.4
	Stem	49.8	25	7.8	15